

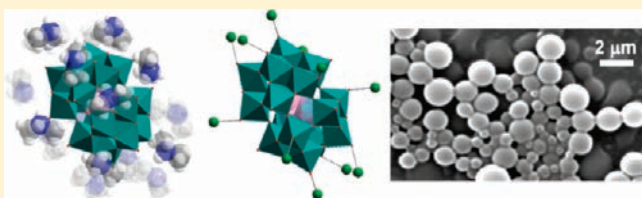
Silver Linked Polyoxometalate Open Frameworks (Ag-POMOFs) for the Directed Fabrication of Silver Nanomaterials

Thomas McGlone, Carsten Streb, Martí Busquets-Fité, Jun Yan, David Gabb, De-Liang Long, and Leroy Cronin*

WestCHEM, School of Chemistry, University of Glasgow, Glasgow G12 8QQ, U.K.

S Supporting Information

ABSTRACT: A design approach for the preparation of the $\{(\text{DMAH})_7[\text{H}_2\text{SbW}_{18}\text{O}_{60}]\}$ (**DMAH-2**) and $\{(\text{DMAH})_7[\text{H}_2\text{BiW}_{18}\text{O}_{60}]\}$ (**DMAH-3**) (**DMAH** = dimethylammonium) systems in a highly pure crystalline form is presented, and the latter is characterized by electrospray ionization mass spectrometry (ESI-MS) methods for the first time. These, together with the archetypal $[\text{W}_{10}\text{O}_{32}]$ cluster, are used as precursors for the formation of unique framework materials incorporating Ag(I) as a linking species. The systems are fully characterized by X-ray crystallography, elemental analysis, IR and thermogravimetric analysis (TGA), and the pyrolysis of the $\{\text{Ag}_4\text{-W}_{10}\text{O}_{32}\}$ system (**1**) leads to the formation of silver microparticles embedded in the resulting tungsten oxide and this has been observed by us previously with other systems. In contrast, the carefully controlled decomposition of the antimony and bismuth systems $\{\text{Ag}_{418}\text{O}_{60}\}$ (**Ag-2**) and $\{\text{Ag}_4\text{-SbW}_{18}\text{O}_{60}\}$ (**Ag-3**) gives rise to the formation of highly pure, discrete silver microparticles as confirmed by powder X-ray diffraction (PXRD), scanning electron microscopy (SEM), and energy dispersive X-ray (EDX) analysis. These unique materials may be interesting for applications such as catalysis, antimicrobial agents, or electroactive/photoactive coatings, and this work demonstrates how the molecular organization of the building blocks on the nanoscale can affect the assembly of materials over a range of length scales.



INTRODUCTION

The design of highly structured nanomaterials has become an important topic with a huge range of important applications rapidly evolving.^{1–4} By using bottom up self-assembly processes on the low nanometer domain (0.5–5 nm) to construct novel systems, and subsequently translating this assembly to the nanoscale, it is effectively possible to develop a new and exciting range of functional nanoarchitectures.^{5,6} Polyoxometalates (POMs) as anionic transition metal oxide clusters^{7,8} are prime candidates for directing the growth of such materials primarily due to fact that discrete clusters can be readily engineered with dimensions of up to 5 nm.⁹ Furthermore, highly organized frameworks can be routinely designed with tailored properties and direct effects of transferring this order and these properties to the micro- and nanoscale have been observed previously.^{10,11}

Over the last five years, our group has developed a comprehensive library of POM-based networks incorporating electrophilic Ag(I) as a linking species due to the high versatility of the transition metal in adopting numerous geometries and coordination numbers.^{12–15} Specifically, the promotion of multiple argentophilic $\text{Ag}\cdots\text{Ag}$ interactions which overcome electrostatic repulsion between formal Ag(I) centers^{16,17} has led to some highly unique systems. The research groups of Sha, Peng, and Mak have also made significant contributions.^{18–22} Of particular interest was the recent fusion of $\{\text{Ag}_3\}$ and $\{\text{Ag}_1\}$ units with $[\text{H}_2\text{V}_{10}\text{O}_{28}]^{4-}$ ($\{\text{V}_{10}\}$) clusters into supramolecular architectures

featuring one-dimensional (1-D) zigzag chains and two-dimensional (2-D) networks.¹¹ We were able to show that these crystalline precursors could be utilized in a novel templating route for the gram scale production of composite semiconducting vanadium oxide nanowires incorporating discrete silver nanoparticles. In this work, the crystalline long-range ordering was essential for nanostructure formation, with analogous amorphous materials failing to produce the nanowires. Very recently, we reported the preparation of extended framework materials incorporating the unique isopolyanion $[\text{H}_4\text{W}_{19}\text{O}_{62}]^{6-}$ ($\{\text{W}_{19}\}$) and using Ag(I) as a linker.²³ We demonstrated that the isomeric form of the initial $\{\text{W}_{19}\}$ cluster had a direct effect on the resulting framework with regard to silver connectivity and crystallographic packing. Furthermore, we were able to show that with direct thermal treatment the selective formation of silver microparticles embedded in the oxide occurred, resulting in the unique formation of pure silver-tungsten oxide materials. A selection of silver-containing POM systems is shown below in Figure 1.

Herein we report the assembly of three novel Ag(I) frameworks based on the archetypal decatungstate cluster $[\text{W}_{10}\text{O}_{32}]^{4-}$ ($\{\text{W}_{10}\}$) and nonclassical Dawson type systems $[\text{SbW}_{18}\text{O}_{60}]^{9-}$

Received: February 24, 2011

Revised: April 10, 2011

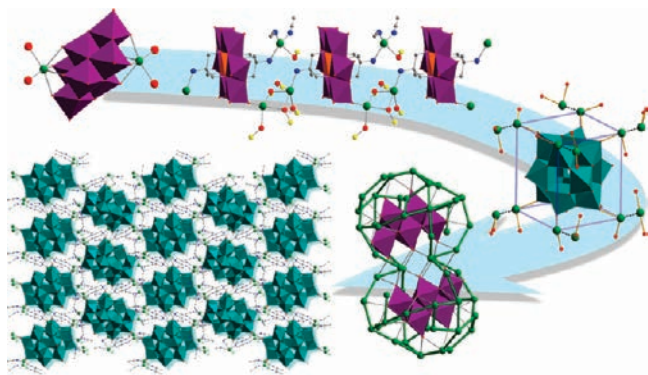


Figure 1. Selection of previously reported POM-based systems utilizing Ag(I) as a linking species. Top left: the $\{\text{Ag}(\text{Mo}_8)\text{Ag}\}^{2-}$ building block,²⁴ top middle: a section of the Mn Anderson cluster linked 1-D chains¹⁴ and top right: a $\{\text{W}_{12}\text{Ag}_5\}$ cube as part of a purely inorganic 3-D framework comprising $[\text{H}_3\text{W}_{12}\text{O}_{40}]^{5-}$ and $\{\text{Ag}_2\}^{2+}$ building blocks with microporous channels.¹⁵ Bottom right: a giant silver alkynyl cage encapsulating two $\{\text{Mo}_6\}$ units.²⁵ $\text{Ag} \cdots \text{Ag}$ contacts shorter than 3.4 Å are drawn as green bonds and tBuC≡C ligands and triflate anions are omitted for clarity. Bottom left: the highly interconnected network resulting from the incorporation of the unique $\{\text{W}_{19}\}$ cluster.²³ W: teal, Mo: purple, Mn: orange polyhedra. O: red, Ag: green, N: blue, C: gray, S: yellow spheres.

and $[\text{BiW}_{18}\text{O}_{60}]^{9-}$ ($\{\text{SbW}_{18}\}$ and $\{\text{BiW}_{18}\}$). The utilization of the highly stable, classical Dawson type clusters $[\text{X}_2\text{M}_{18}\text{O}_{62}]^{p-}$ (where M = Mo, W; X = P, S, etc.) as building blocks for the formation of extended framework materials has been extensively reported of late, with many examples featured across the literature.^{26–28} Of considerably less attention are the nonclassical types, where the two central tetrahedral groups of the Dawson cluster are replaced by a single pyramidal (AsO_3^{3-} , SbO_3^{3-} , BiO_3^{3-}),^{29–31} a single tetrahedral (PO_4^{3-} , AsO_4^{3-}),³² two pyramidal (SO_3^{2-}),^{33,34} or a single octahedral (IO_6^{5-} , WO_6^{6-} , NaF_6^{5-})^{35–37} group. The presently discussed $\{\text{W}_{10}\}$ system features a highly interconnected, 2-D array of cluster sheets aligned infinitely in the third dimension with the overall formula $(\text{Ag}(\text{CH}_3\text{CN})_3)_2(\text{Ag}(\text{CH}_3\text{CN})_2)_2[\text{W}_{10}\text{O}_{32}]$ (**1**). Pyrolysis of this system at elevated temperatures gives rise to a material comprising silver microparticles of the size range ca. 2–30 μm embedded in a tungsten oxide matrix, almost completely analogous to the previously mentioned $\{\text{W}_{19}\}$ system. The frameworks based on $\{\text{SbW}_{18}\}$ and $\{\text{BiW}_{18}\}$ are essentially isostructural with respective formulas $(\text{Ag}(\text{CH}_3\text{CN})_3)_2(\text{Ag}(\text{CH}_3\text{CN})_2)_2[\text{H}_5\text{SbW}_{18}\text{O}_{60}] \cdot 2\text{CH}_3\text{CN}$ (**Ag-2**) and $(\text{Ag}(\text{CH}_3\text{CN})_3)_2(\text{Ag}(\text{CH}_3\text{CN})_2)_2[\text{H}_5\text{BiW}_{18}\text{O}_{60}] \cdot 2\text{CH}_3\text{CN}$ (**Ag-3**). The arrangement in the solid state is intrinsically complex with the cluster units stacked in infinite, linear pillars which in turn are arranged in a hexagonal fashion giving rise to a highly unique structural system. Direct treatment of these crystalline materials with a concentrated solution of sodium hydroxide gives rise to a distinctive array of pure silver microparticles with a nonuniform size distribution in the range of 1–10 μm.

RESULTS AND DISCUSSION

The $\{\text{W}_{10}\}$ cluster comprises 10 fully oxidized W^{VI} centers and can be simply rationalized as two edge-sharing $\{\text{W}_5\}$ units fused together via four corner-sharing positions. A major attraction of this unit for the purposes of constructing supramolecular

framework materials is its ease of preparation on a multigram scale, and hence it is reasonable to expect that any resulting architectures could also be prepared on such a level. The reaction of $(\text{TBA})_4[\text{W}_{10}\text{O}_{32}]$ (TBA = *n*-tetrabutylammonium) with silver(I) nitrate in acetonitrile resulted in the formation of colorless platelike crystals which were analyzed by single crystal X-ray diffraction (see Table 1), and this, in combination with flame atomic absorption spectroscopy (FAAS), greatly assisted in determination of the formula. Investigation of the crystal structure revealed that the $\{\text{W}_{10}\}$ building unit is coordinated to six silver(I) centers in a pseudo octahedral fashion; see Figure 2. Ag positions A and A' located at the top and bottom of the cluster unit are slightly disordered over two sites and are connected via terminal oxygen ligands with a distance $d_{\text{O}-\text{Ag}} = 2.60\text{--}2.75$ Å. These square planar centers act as linking points to neighboring clusters and their coordination spheres are filled by two acetonitrile molecules. Ag positions B and B' feature a $d_{\text{O}-\text{Ag}}$ distance of 2.555(5) Å and do not link to adjacent clusters but instead act as capping groups with three coordinated acetonitrile ligands arranged in an overall tetrahedral environment. The remaining Ag centers (C and C') are located at the sides of the $\{\text{W}_{10}\}$ cluster unit and are each coordinated to two terminal oxygen positions with distances $d_{\text{O}-\text{Ag}} = 2.760(5)$ and 2.850(5) Å. These centers also accommodate linkage to neighboring cluster units and contain two additional acetonitrile ligands, completing the disordered octahedral coordination sphere.

In the crystal lattice of **1**, the clusters are not observed as discrete units but are linked into 2-D sheets via silver(I) centers A and A' at the top and bottom of the cluster and silver(I) centers C and C' located at each side. In the third dimension, these 2-D sheets are stacked directly on top of each other so that an infinite arrangement is established. The shortest $\text{Ag} \cdots \text{Ag}$ distance in the framework structure is 3.843(5) Å, which lies outside the van der Waals radii distance, and hence indicates no additional stability from favorable argentophilic interactions. As originally predicted, it is possible to readily prepare system **1** in high yield and on a multigram scale. Upon thermal treatment under an atmosphere of nitrogen, all the acetonitrile ligands can be removed and thermogravimetric analysis (TGA) shows that this is complete by ~200 °C (see Supporting Information). The calculated and experimental values for solvent removal are 12.8 and 11.8% respectively, the discrepancy attributed to premature solvent evaporation during sample preparation. Further weight loss was observed as temperatures of ~300 °C were exceeded, indicating some structural rearrangements of the cluster. These were investigated by variable temperature powder X-ray diffraction (PXRD) yielding highly informative results. By comparing patterns obtained from a crystal structure simulation of **1**³⁸ and a room temperature data collection of freshly prepared, well ground crystals, a suitable match was obtained; see Figure 3. Furthermore, it was observed that at temperatures exceeding 350 °C, the formation of face-centered cubic (FCC) silver metal occurs, and this can be definitively matched to its simulated pattern also displayed in Figure 3.

The PXRD results indicate the formation of robust silver-tungsten oxide materials due to the assignment of FCC silver metal and various forms of tungsten oxide using the ICDD database. It was decided to investigate further by studying scanning electron microscopy (SEM) images at the sub-micro- and nanometer scale. A summary of the striking images obtained is displayed below in Figure 4. The thermal treatment of **1** under a nitrogen atmosphere to temperatures exceeding ~350 °C

Table 1. Crystallographic Data for All Compounds

	1	DMAH-2	TBA-2	Ag-2	DMAH-3	TBA-3	Ag-3
formula	C ₂₀ H ₃₀ Ag ₄ ⁻ N ₁₀ O ₃₂ W ₁₀	C ₁₄ H ₇₀ N ₇ ⁻ O ₆₆ SbW ₁₈	C ₇₆ H ₁₇₉ N ₁₀ ⁻ O ₆₀ SbW ₁₈	C ₂₄ H ₄₁ Ag ₄ ⁻ N ₁₂ O ₆₀ SbW ₁₈	C ₁₄ H ₈₀ ⁻ BiN ₇ O ₇₁ W ₁₈	C ₈₆ H ₂₀₁ ⁻ BiN ₈ O ₆₀ W ₁₈	C ₂₄ H ₄₁ Ag ₄ ⁻ BiN ₁₂ O ₆₀ W ₁₈
M _r [g mol ⁻¹]	3192.5	4823.82	5624.34	5320.22	5001.13	5825.83	5407.45
system	triclinic	monoclinic	triclinic	trigonal	triclinic	tetragonal	trigonal
group	P $\bar{1}$	P2(1)/n	P $\bar{1}$	R $\bar{3}c$	P $\bar{1}$	I4	R $\bar{3}c$
a [Å]	11.2492(2)	13.318(3)	16.5543(3)	20.5131(2)	12.8261(6)	42.0448(3)	20.5547(9)
b [Å]	11.3536(3)	23.362(5)	20.5284(3)	20.5131(2)	13.0348(5)	42.0448(3)	20.5547(9)
c [Å]	13.3378(8)	23.198(5)	22.6908(3)	33.4645(5)	13.3700(5)	15.6967(2)	33.1479(19)
α [°]	65.508(3)	90	92.7760(10)	90	73.647(3)	90	90
β [°]	81.846(6)	95.652(9)	109.4300(10)	90	61.499(4)	90	90
γ [°]	60.791(2)	90	108.9400(10)	120	89.952(3)	90	120
ρ _{calcd} [g cm ⁻³]	3.929	4.461	2.758	4.347	4.462	2.785	4.438
V [Å ³]	1349.17(9)	7182(3)	6771.66(18)	12194.9(2)	1861.13(13)	27748.1(5)	12128.5(10)
Z	1	4	2	6	1	8	6
μ(MoKα) [mm ⁻¹]	22.720	29.177	15.493	56.640 (CuKα)	30.157	16.198	28.699
T [K]	150(2)	100(2)	150(2)	150(2)	150(2)	150(2)	150(2)
rfins (meas) (measd)	17028	51609	112087	23901	16580	67927	23492
rfins (uniq)	4985	12289	25681	2433	6883	24826	2514
no. params	350	675	955	158	443	1003	174
R1 (I > 2σ(I))	0.0255	0.0415	0.0394	0.0453	0.0320	0.0389	0.0543
wR2 (all)	0.0609	0.0816	0.1085	0.1321	0.0801	0.0787	0.1327

yields a unique material comprising silver microparticles of the size range ca. 2–30 μm embedded in a tungsten oxide matrix. Energy dispersive X-ray (EDX) analysis was also used to confirm the composition of the material following thermal treatment. As there is no other electron source due to the {W₁₀} cluster being fully oxidized, it is postulated that the Ag(I) centers on the initial cluster units are reduced to Ag(0) as electrons are released from framework oxygen ligands, which are then eliminated as molecular oxygen.

The {SbW₁₈} anion was first presented by Krebs et al. in 1994,²⁹ but the crystal structure was only reported quite recently,^{39,40} establishing the presence of a single Sb(III) center within the cluster cage and this was proved unambiguously with electrospray ionization mass spectrometry (ESI-MS) studies. The Bi(III) analogue was originally reported by Sasaki et al. in 1987³¹ and featured less general ambiguity because the larger size of the Bi(III) center definitively does not allow for the encapsulation of two heteroatoms within a single Dawson cage. The synthetic methods for the {SbW₁₈} and {BiW₁₈} systems are somewhat limited across the literature in terms of purity and reproducibility and one particular problem is an additional cluster byproduct which is formed under almost identical conditions, namely, [X^{III}₂W₂₂O₇₆]¹⁴⁻.^{41,42} Therefore, it was initially essential to establish suitable procedures for the preparation of the {SbW₁₈} and {BiW₁₈} clusters as TBA salts. A synthetic strategy was devised whereby the clusters could be obtained in high yield, and more importantly high purity, in a one-pot reaction. By continuing the theme of structural direction from organic templates which allowed the isolation of such systems as [H₄W₁₉O₆₂]⁶⁻ and [H₁₂W₃₆O₁₂₀]¹²⁻,^{36,43–45} protonated dimethylamine (DMAH) was employed in a boiling aqueous reaction medium with sodium tungstate and antimony(III) oxide at pH 3.6, and subsequent crystallization yielded a new species, (DMAH)₇[H₂SbW₁₈O₆₀]·6 H₂O (DMAH-2). This synthetic approach proved highly effective in obtaining the {SbW₁₈} cluster in a pure crystalline

form and high yield. Once this had been achieved, cation exchange with a TBA salt can be performed to maximize solubility in organic solvents and a mixed DMAH and TBA salt could be obtained: (DMAH)₃(TBA)₄[H₂SbW₁₈O₆₀]·3CH₃CN (TBA-2). Residual DMAH cations are present due to the steric constraints of additional bulky TBA molecules. Analogous synthetic procedures were performed in order to obtain the bismuth equivalents: (DMAH)₇[H₂BiW₁₈O₆₀]·11H₂O (DMAH-3) and (DMAH)₂(TBA)₅[H₂BiW₁₈O₆₀]·CH₃CN (TBA-3). Although detailed analysis of the {SbW₁₈} cluster via MS methods has been published elsewhere,⁴⁰ to the best of our knowledge equivalent studies on the {BiW₁₈} analogue have not yet been reported. We were able to identify {(TBA)₃[H₃BiW₁₈O₆₀]}³⁻, {(TBA)₃[H₄BiW₁₈O₆₀]}²⁻, and {(TBA)₄[H₃BiW₁₈O₆₀]}²⁻ fragments unambiguously and the results are summarized in the Supporting Information.

The reaction of TBA-2 and TBA-3 with silver(I) nitrate in acetonitrile in the presence of aqueous HNO₃ yielded the two novel, intrinsically complex framework materials Ag-2 and Ag-3. Complete crystal structures were obtained for each (see Table 1) in addition to a full elemental analysis, and thermal studies were also completed showing the loss of all solvent and coordinated acetonitrile molecules; see Supporting Information. The following structural description will be focused on the {SbW₁₈} system which is essentially isostructural with that of {BiW₁₈}. Framework 2 crystallizes in the trigonal system and is highly symmetric with only one-sixth of a {SbW₁₈} cluster comprising the asymmetric unit. Each cluster is formally coordinated to 12 silver centers, three at the top with bond distance $d_{O-Ag} = 2.633(10)$ Å, three at the bottom ($d_{O-Ag} = 2.635(10)$ Å), and six around the sides with three distances $d_{O-Ag} = 2.580(10)$ Å and three with $d_{O-Ag} = 2.581(10)$ Å. None of these centers are fully occupied; in fact each features an occupancy of ca. 0.3 with the exception of those highlighted in blue in Figure 5 which have an occupancy of less than 0.1. These sites are located in the center of the triangular array of Ag positions above and below the cluster units and

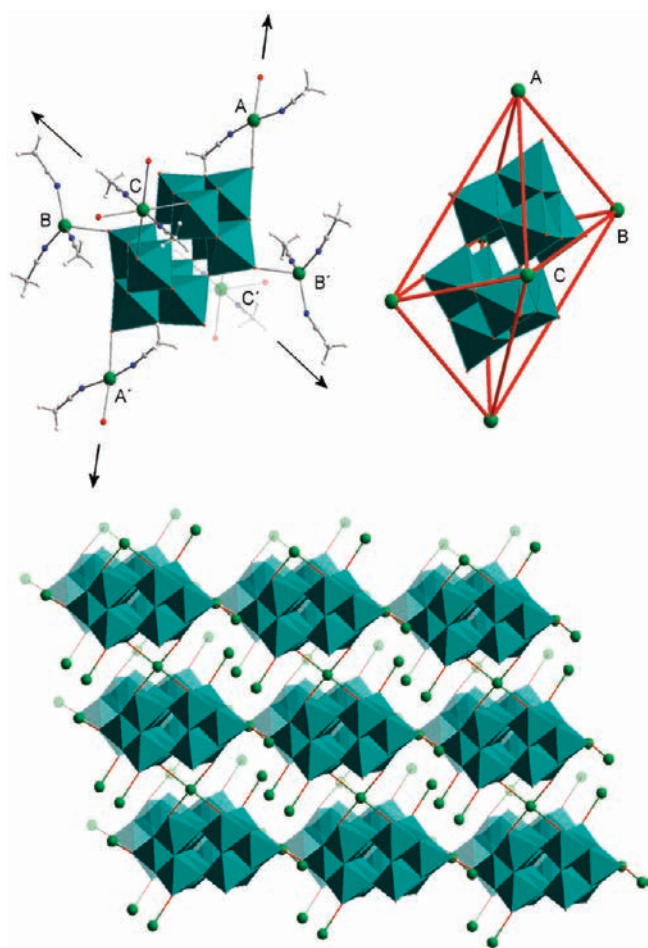


Figure 2. Representation of **1**. Top left: a single cluster unit showing all Ag connectivity including coordinated acetonitrile molecules. Top right: schematic rationalizing the Ag positions as a distorted octahedral cage around the $\{W_{10}\}$ unit. This is shown by imaginary, elongated red bonds. Bottom: the crystallographic packing of the system, viewing along the crystallographic b -axis, with all solvent molecules omitted for clarity. The Ag(I) centers are labeled A, A', B, B', C, C' and the A and C type positions allow connection to adjacent cluster units. W: teal polyhedra, Ag: green, C: gray, N: blue and H: white spheres.

feature a short distance of $d_{Ag-Ag} = \text{ca. } 2.68 \text{ \AA}$, which, being shorter than the distance for a metallic Ag–Ag bond (ca. 2.89 \AA) are a clear indication of disordered Ag positions. Because of the high level of silver disorder in the overall system, it is difficult to specify exactly the nature of the $Ag \cdots Ag$ interactions within the framework. An initial observation of the distances between adjacent clusters (marked as broken black bonds between silver centers colored green in Figure 5) is a distance of $3.148(4) \text{ \AA}$ indicating significant $Ag \cdots Ag$ interactions; however, due to the disordered nature of the silver centers, this observation should be accepted with caution. It is interesting however to note that three additional protons have been picked up by the cluster units in systems **Ag-2** and **Ag-3** in going from the diprotonated starting materials $[H_2SbW_{18}O_{60}]^{7-}$ and $[H_2BiW_{18}O_{60}]^{7-}$ to the pentaprotonated products $[H_5SbW_{18}O_{60}]^{4-}$ and $[H_5BiW_{18}O_{60}]^{4-}$. As it is not possible for all five protons to be located on internal positions of the cluster units, it is highly likely that the surplus hydrogen atoms are located on external sites. This versatile ability

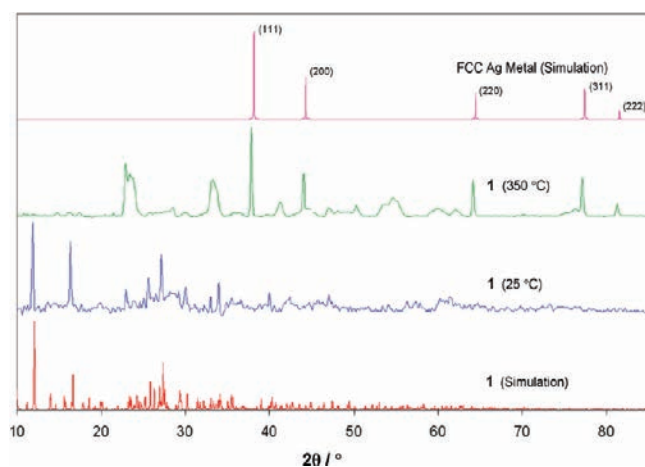


Figure 3. PXRD patterns for compound **1**. The bottom pattern in red was simulated from the crystal structure and the next pattern shown in blue was collected at room temperature using freshly prepared, well ground crystals. These patterns feature a good match. The third pattern from the bottom, shown in green, was collected following heating under nitrogen to $350 \text{ }^\circ\text{C}$, and the top pattern shown in pink is a simulation for face-centered cubic (FCC) silver metal. The signals have been assigned to the corresponding diffraction (hkl) planes.

of the POM cluster to adopt varying protonation states is crucial for the successful formation of complex frameworks **Ag-2** and **Ag-3**, and experiments without the addition of aqueous HNO_3 did not permit successful formation.

The position of the heavy atom cluster units is unambiguous, and investigation of the crystal packing in the lattice reveals a relatively unusual 3-D supramolecular arrangement. The $\{SbW_{18}\}$ clusters are stacked in linear, infinite pillars via a series of $W-O-Ag$ bonds on the top and bottom of each and this is clearly demonstrated in Figure 5. Each pillar is further coordinated to six others via short contact $Ag \cdots Ag$ interactions from the silver(I) centers connected to the sides of the cluster units. The pillars are not directly aligned with each other as the top of one adjacent cluster is in line with the silver centers coordinated to the side of the next. The net effect is an extremely highly coordinated array of $\{SbW_{18}\}$ secondary building units stabilized by short contact $Ag \cdots Ag$ interactions. The coordination sphere of each silver center is filled with two solvent acetonitrile molecules with the exception of the center occupying the midpoint of the triangular array above and below each cluster unit with the low occupancy of less than 0.1. Framework **Ag-2** is only the second reported example of a 3-D framework based on $\{SbW_{18}\}$ polyoxoanions,³⁹ and until now there has only ever been one example of a silver linked tungstobismuthate,⁴⁶ illustrating the highly unique nature of these systems.

The framework **1** and those obtained previously with the $[H_4W_{19}O_{62}]^{6-}$ cluster were completely unique in that they contained no additional heteroatom constituents and hence the resulting materials from pyrolysis comprised a pure silver-tungsten oxide nature. In the case of frameworks **Ag-2** and **Ag-3**, this is not the case, and any similar resulting materials will most certainly contain bismuth or antimony components. Indeed, the standard thermal treatment of **Ag-2** and **Ag-3** did not yield any noticeable structural effects, and to that end, a strategy was devised which induced simultaneous decomposition and removal of the resultant bulk material in addition

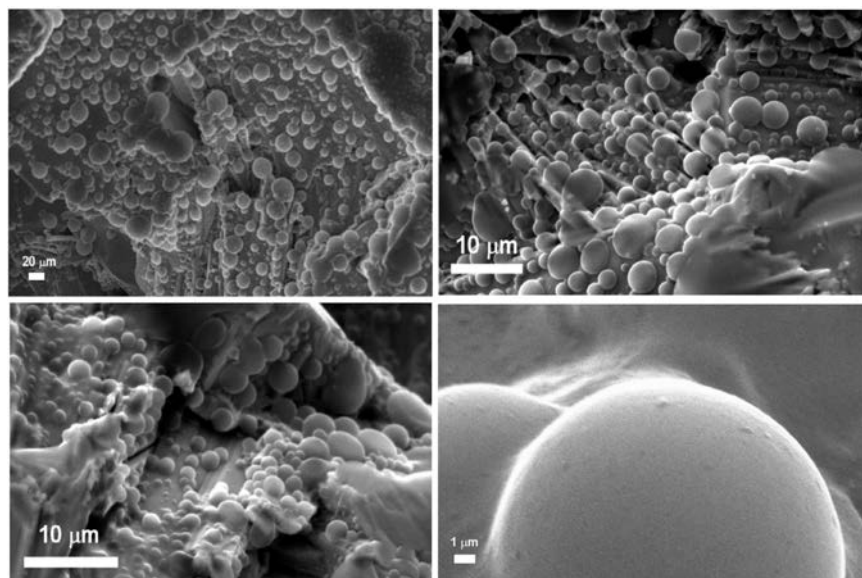


Figure 4. SEM micrographs of compound **1** following heating under nitrogen to 1000 °C. The silver microparticles can be observed with a nonuniform size distribution varying from ca. 2–30 μm.

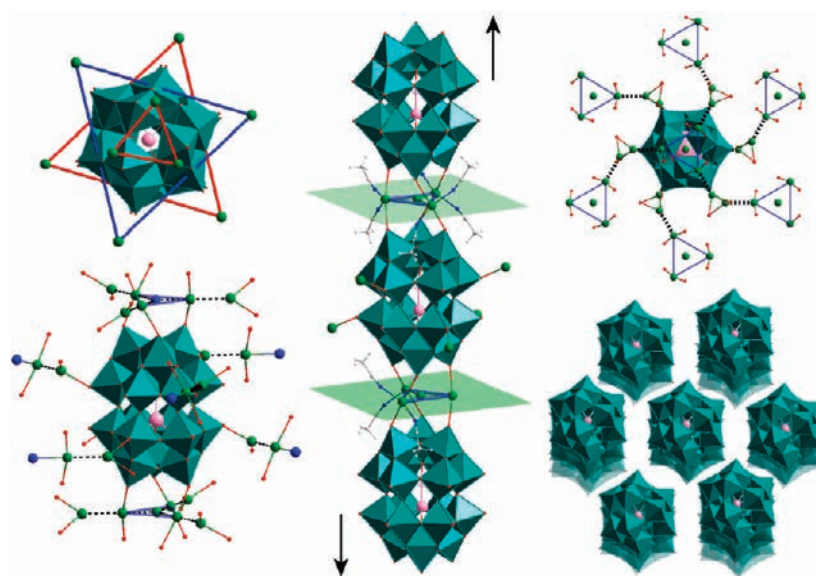


Figure 5. Rationalization of systems **Ag-2** and **Ag-3**. Top left: a single cluster with a schematic showing all coordinated Ag(I) positions. The blue and red triangles highlight these positions clearly. Middle: three cluster units arranged in a pillarlike fashion showing how the Ag coordination extends from the top and bottom of each individual cluster. Top right: Schematic displaying the positions of adjacent cluster-based pillars, with each blue triangle representing a single pillar. Bottom left: A single cluster with all possible short contact Ag(I)···Ag(I) interactions. The disordered Ag atom at the center of each triangular cluster cap is highlighted in blue. Bottom right: the packing arrangement viewing along the crystallographic *c*-axis is shown. W: teal polyhedra, Sb/Bi: pink, Ag: green, C: gray, H: white, N: blue, O: red spheres. Note that the Sb/Bi heteroatom is disordered over two positions and only one is formally encapsulated within each cluster unit.

to reduction of the Ag(I) centers. Treatment of crystals of compounds **Ag-2** and **Ag-3** with strong base (ca. 10 M NaOH solution) yielded materials **Ag-2'** and **Ag-3'** with a composition of predominantly silver as confirmed by EDX analysis and PXRD; see Figure S10 in the Supporting Information. This transformation is completely instantaneous with a rapid color change of pale green to black observed when the base is added. It is most likely that the reducing agent is sodium hydroxide; in this case however there is also a potential

electron source due to the release of molecular oxygen with the collapse of the POM framework as with the $\{W_{10}Ag\}$ system (**1**). Furthermore, on studying SEM images of **Ag-3'**, it can be seen that an ordered array of pure silver microparticles with a nonuniform size distribution in the range of 1–10 μm has formed; see Figure 6. Such a highly organized arrangement has not been observed for **Ag-2'** so far; however, EDX and PXRD studies suggest that both materials feature a similar composition.

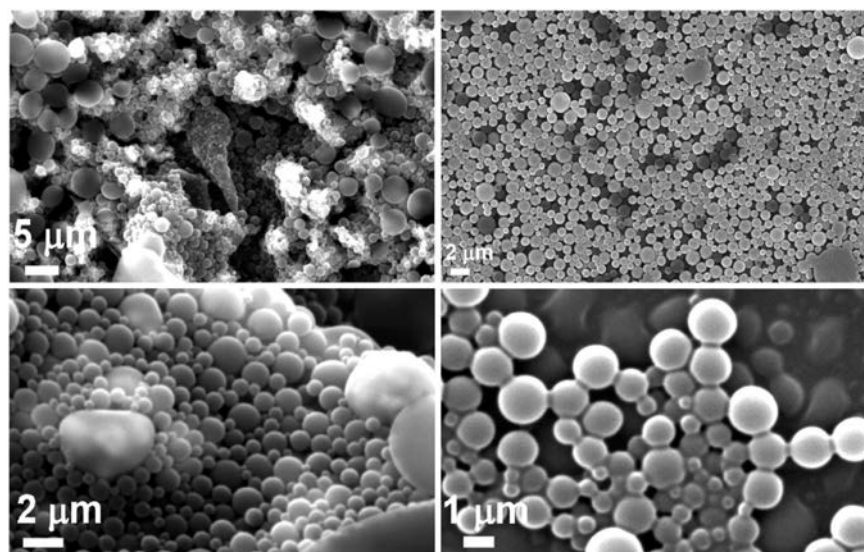


Figure 6. SEM images of Ag-3'. The mixed size distribution of the silver microparticles lies in the range of 1–10 μm .

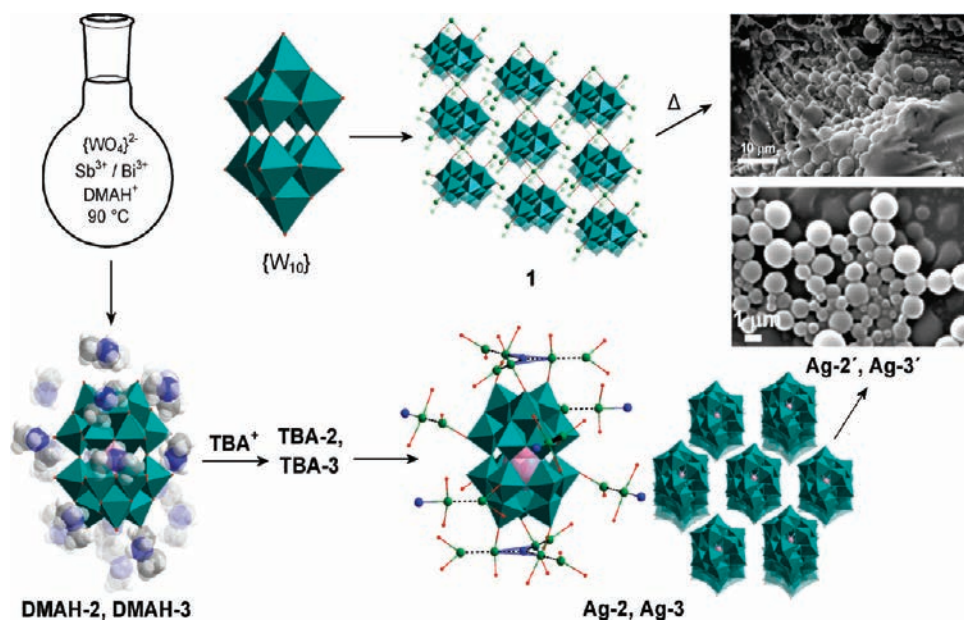


Figure 7. A summary of all the systems discussed. Top right scheme: the archetypal decatungstate cluster $\{W_{10}\}$ is incorporated into a 2-D network and subsequent pyrolysis leads to silver sub-microparticles embedded in the resulting oxide. Bottom scheme: TBA salts of the $\{SbW_{18}\}$ and $\{BiW_{18}\}$ clusters are prepared via a novel synthetic route by first isolating as DMAH salts. The clusters are then incorporated into 3-D silver networks which are isostructural. Subsequent treatment with base results in the formation of highly pure silver microparticles with a nonuniform size distribution. W: teal polyhedral, Sb/Bi: pink, Ag: green, O: red, N: blue, C: gray, H: white spheres.

CONCLUSIONS

In summary, we have presented a novel synthetic approach for the preparation of the $\{SbW_{18}O_{60}\}^{9-}$ and $\{BiW_{18}O_{60}\}^{9-}$ systems in a highly pure crystalline form. The latter has also been characterized by ESI-MS methods for the first time. Together with the archetypal $\{W_{10}O_{32}\}^{4-}$ unit, these clusters were then used as precursors for the formation of extended framework materials incorporating Ag(I) as a linking species. Six silver centers encapsulate the $\{W_{10}\}$ unit in resemblance to a distorted octahedron, and this allows linking of the clusters into an infinite array of 2-D sheets. The $\{SbW_{18}\}$ and $\{BiW_{18}\}$ systems gave rise

to highly unique structural architectures with the cluster units arranged “head to tail” in infinite pillars. These pillars are further arranged in a vast hexagonal array with additional stabilization from short contact $Ag \cdots Ag$ interactions. The $\{SbW_{18}\}$ framework is only the second reported example of a 3-D framework based on this cluster anion, and until now there has only ever been one example of a silver linked tungstobismuthate. Furthermore, the pyrolysis of the novel $\{Ag_4W_{10}O_{32}\}$ -based system led to the formation of silver microparticles embedded in the resulting tungsten oxide, completely analogous to the previously reported silver-containing systems based on the unique $\{H_4W_{19}O_{62}\}^{6-}$

cluster. The carefully controlled decomposition of the silver-containing antimony and bismuth systems instead gave rise to a highly pure arrangement of discrete silver microparticles as confirmed by PXRD, SEM, and EDX analysis. A summary of all the systems is displayed below in Figure 7. Future work will involve the exploitation of these materials in areas such as catalysis, antimicrobial agents, or electroactive/photoactive coatings.

EXPERIMENTAL SECTION

All reagents and chemicals were supplied by Sigma Aldrich Chemical Co. Ltd. and used without further purification. The $(\text{TBA})_4[\text{W}_{10}\text{O}_{32}]$ precursor (TBA = *n*-tetrabutylammonium) was synthesized according to the literature procedure.⁴⁷ $\{\text{SbW}_{18}\}$ and $\{\text{BiW}_{18}\}$ precursors were prepared using adapted methods to those reported previously.^{31,40} DMAH = protonated dimethylamine. X-ray structure analysis and crystallographic data: suitable single crystals of **1**, **DMAH-2**, **TBA-2**, **Ag-2**, **DMAH-3**, **TBA-3**, and **Ag-3** were selected and mounted onto the end of a thin glass fiber using Fomblin oil. Structure solution and refinement was carried out with SHELXS-97⁴⁸ and SHELXL-97⁴⁸ using WinGX.⁴⁹

Preparation of $(\text{Ag}(\text{CH}_3\text{CN})_3)_2(\text{Ag}(\text{CH}_3\text{CN})_2)[\text{W}_{10}\text{O}_{32}]$ (1**).** $(\text{TBA})_4[\text{W}_{10}\text{O}_{32}]$ (500 mg, 0.15 mmol) was dissolved in warm acetonitrile (50 mL) and AgNO_3 (390 mg, 2.30 mmol) dissolved in acetonitrile (5 mL) was added all at once to the stirring mixture. This was stirred for 24 h with the vessel sealed. Following centrifugation to remove insoluble material, diffusion of diethyl ether yielded square colorless crystals after ca. 3 days. Yield: 0.34 g, 0.11 mmol, 73.3% yield based on $(\text{TBA})_4[\text{W}_{10}\text{O}_{32}]$. Elemental analysis, (dried material) in wt-% for $\text{Ag}_4\text{O}_{32}\text{W}_{10}$ (calculated values in brackets): Ag: 15.5 (15.5), W: 66.0 (66.1). Elemental analysis in wt% for $\text{C}_{20}\text{H}_{30}\text{N}_{10}\text{Ag}_4\text{O}_{32}\text{W}_{10}$ (calculated values in brackets): C: 7.4 (7.5), H: 0.9 (1.0), N: 4.2 (4.4).

Preparation of $(\text{DMAH})_7[\text{H}_2\text{SbW}_{18}\text{O}_{60}] \cdot 6 \text{H}_2\text{O}$ (DMAH-2**).** $\text{Na}_2\text{WO}_4 \cdot 2\text{H}_2\text{O}$ (13.2 g, 40.0 mmol) was dissolved in water (50 mL) and heated to 90 °C. $\text{DMA} \cdot \text{HCl}$ (2.0 g, 24.53 mmol) was added to the tungstate solution. Sb_2O_3 (0.50 g, 1.72 mmol) dissolved in 4 M HCl (15 mL) was then added dropwise to the tungstate solution over a period of 2 min. The solution pH was adjusted and kept at 3.6 using 4 M HCl, while the temperature was maintained at 90 °C for 10 min. The mixture was then allowed to cool to room temperature and filtered to remove insolubles. After ca. 5 days standing in an open flask, small pale green block crystals began to appear. These were collected via filtration and washed with a minimal amount of very cold water. Yield: 2.90 g, 0.60 mmol, 27.0% based on tungsten. Elemental analysis, (dried material) in wt% for $\text{C}_{14}\text{H}_{58}\text{N}_7\text{O}_{60}\text{SbW}_{18}$ (calculated values in brackets): C: 3.2 (3.6), H: 1.0 (1.2), N: 2.0 (2.1).

Preparation of $(\text{DMAH})_3(\text{TBA})_4[\text{H}_2\text{SbW}_{18}\text{O}_{60}] \cdot 3\text{CH}_3\text{CN}$ (TBA-2**).** Freshly prepared crystals of $(\text{DMAH})_7[\text{H}_2\text{SbW}_{18}\text{O}_{60}] \cdot 6\text{H}_2\text{O}$ (2.0 g, 0.41 mmol) were dissolved in water (20 mL) and the pH was readjusted to 3.6 with 4 M HCl. $\text{TBA} \cdot \text{Br}$ (2.5 g, 7.76 mmol) dissolved in water (15 mL) was added to the solution, and the resulting white precipitate was stirred for 10 min, collected by filtration, and washed sequentially with plenty of H_2O and Et_2O . The solid was then dried in a vacuum. Yield: 1.80 g, 0.33 mmol, 80.5% based on $(\text{DMAH})_7[\text{H}_2\text{SbW}_{18}\text{O}_{60}] \cdot 6\text{H}_2\text{O}$. Elemental analysis, (dried material) in wt% for $\text{C}_{70}\text{H}_{170}\text{N}_7\text{O}_{60}\text{SbW}_{18}$ (calculated values in brackets): C: 15.7 (15.3), H: 3.1 (3.1), N: 1.6 (1.8). Crystals suitable for single crystal diffraction were obtained by recrystallization from a minimal amount of acetonitrile and diethyl ether diffusion. The crystallographic formula includes three solvent acetonitrile molecules.

Preparation of $(\text{Ag}(\text{CH}_3\text{CN})_3)_2(\text{Ag}(\text{CH}_3\text{CN})_2)[\text{H}_5\text{SbW}_{18}\text{O}_{60}] \cdot 2\text{CH}_3\text{CN}$ (Ag-2**).** A freshly prepared, dried sample of $(\text{TBA})_4(\text{DMAH})_3[\text{H}_2\text{SbW}_{18}\text{O}_{60}]$ (0.50 g, 0.09 mmol) was dissolved in warm CH_3CN (50 mL). AgNO_3 (0.18 g, 1.06 mmol) was dissolved in CH_3CN (10 mL) and added dropwise to the mixture. 1.5 mL of 2 M HNO_3 was then added.

The resulting mixture was heated under reflux overnight at 90 °C with stirring. After allowing it to cool the reaction mixture was centrifuged and filtered to remove insoluble material. Colorless, block crystals were obtained by diffusion of EtOAc after ca. 5 days and collected by filtration. Yield: 90 mg, 16.9 μmol , 18.8% based on $(\text{TBA})_4(\text{DMAH})_3[\text{H}_2\text{SbW}_{18}\text{O}_{60}]$. Elemental analysis, (loss of seven acetonitrile molecules), in wt% for $\text{C}_{10}\text{H}_{20}\text{Ag}_4\text{N}_5\text{O}_{60}\text{SbW}_{18}$ (calculated values in brackets): Ag: 7.6 (8.6), Sb: 2.2 (2.4), W: 66.6 (65.8). Elemental analysis, (loss of four acetonitrile molecules), in wt-% for $\text{C}_{16}\text{H}_{29}\text{N}_8\text{Ag}_4\text{O}_{60}\text{SbW}_{18}$ (calculated values in brackets): C: 3.7 (3.7), H: 0.7 (0.6), N: 2.5 (2.2).

Ag-2' was prepared by adding ca. 100 mg of crystals of **Ag-2** to ca. 1 mL of 10 M NaOH solution. The color change from pale green to black was instantaneous and the mixture was sonicated briefly to ensure all the crystals had reacted. The resultant black material was washed three times with water, twice with ethanol, and dried in a vacuum.

Preparation of $(\text{DMAH})_7[\text{H}_2\text{BiW}_{18}\text{O}_{60}] \cdot 11 \text{H}_2\text{O}$ (DMAH-3**).** $\text{Na}_2\text{WO}_4 \cdot 2 \text{H}_2\text{O}$ (18.8 g, 57.0 mmol) was dissolved in water (100 mL) and heated to 90 °C. $\text{DMA} \cdot \text{HCl}$ (2.5 g, 30.66 mmol) was added to the tungstate solution. Bi_2O_3 (1.10 g, 2.36 mmol) dissolved in 4 M HCl (15 mL) was then added dropwise to the tungstate solution over a period of 2 min. The solution pH was adjusted and kept at 2.0 using 4 M HCl while the temperature was maintained at 90 °C for 20 min. The mixture was stirred overnight and allowed to cool to room temperature, then centrifuged and filtered to remove insoluble material. After ca. 2 weeks standing in an open flask, small pale green block crystals began to appear. These were collected via filtration and washed with a minimal amount of very cold water. Yield: 3.50 g, 0.70 mmol, 22.1% based on tungsten. Elemental analysis, (dried material) in wt% for $\text{C}_{14}\text{H}_{58}\text{N}_7\text{BiO}_{60}\text{W}_{18}$ (calculated values in brackets): C: 3.0 (3.5), H: 1.1 (1.2), N: 1.8 (2.0).

Preparation of $(\text{DMAH})_2(\text{TBA})_5[\text{H}_2\text{BiW}_{18}\text{O}_{60}] \cdot \text{CH}_3\text{CN}$ (TBA-3**).** Freshly prepared crystals of $(\text{DMAH})_7[\text{H}_2\text{BiW}_{18}\text{O}_{60}] \cdot 11\text{H}_2\text{O}$ (2.0 g, 0.40 mmol) were dissolved in water (20 mL) and the pH was adjusted to 2.0 with 4 M HCl. $\text{TBA} \cdot \text{Br}$ (2.5 g, 7.76 mmol) dissolved in water (15 mL) was added to the solution and the resulting white precipitate was stirred for 10 min, collected by filtration, and washed sequentially with plenty of H_2O and Et_2O . The solid was also dried in a vacuum. Yield: 2.10 g, 0.36 mmol, 90.0% based on $(\text{DMAH})_7[\text{H}_2\text{BiW}_{18}\text{O}_{60}] \cdot 11 \text{H}_2\text{O}$. Elemental analysis, (dried material), in wt% for $\text{C}_{84}\text{H}_{198}\text{N}_7\text{BiO}_{60}\text{W}_{18}$ (calculated values in brackets): C: 17.2 (17.4), H: 3.4 (3.5), N: 1.5 (1.7). Crystals suitable for single crystal diffraction were obtained by recrystallization from a minimal amount of acetonitrile and diethyl ether diffusion. The crystallographic formula includes three solvent acetonitrile molecules. For ESI-MS studies compound **TBA-3** was recrystallized from acetonitrile and the resulting highly pure material was redissolved in acetonitrile and diluted so that the maximum concentration of the cluster ions was of the order 10^{-4} M and this was injected into the instrument.

Preparation of $(\text{Ag}(\text{CH}_3\text{CN})_3)_2(\text{Ag}(\text{CH}_3\text{CN})_2)[\text{H}_5\text{BiW}_{18}\text{O}_{60}] \cdot 2\text{CH}_3\text{CN}$ (Ag-3**).** A freshly prepared, dried sample of $(\text{DMAH})_2(\text{TBA})_5[\text{H}_2\text{BiW}_{18}\text{O}_{60}]$ (0.50 g, 0.09 mmol) was dissolved in warm CH_3CN (50 mL). AgNO_3 (0.18 g, 1.06 mmol) dissolved in CH_3CN (10 mL) was added dropwise to the first mixture. Two milliliters of 2 M HNO_3 was subsequently added, and the mixture was heated under reflux conditions at 90 °C overnight. The mixture was then centrifuged and filtered and allowed to cool to room temperature. Colorless block crystals were obtained by EtOAc diffusion after ca. 5 days and collected by filtration. Yield: 150 mg, 27.7 μmol , 30.8% based on $(\text{DMAH})_2(\text{TBA})_5[\text{H}_2\text{BiW}_{18}\text{O}_{60}]$. Elemental analysis, in wt% for $\text{C}_{24}\text{H}_{41}\text{N}_{12}\text{Ag}_4\text{BiO}_{60}\text{W}_{18}$ (calculated values in brackets): Ag: 7.6 (8.0), Bi: 4.2 (3.9), W: 59.4 (61.2). Elemental analysis, (loss of four acetonitrile molecules), in wt% for $\text{C}_{16}\text{H}_{29}\text{N}_8\text{Ag}_4\text{BiO}_{60}\text{W}_{18}$ (calculated values in brackets): C: 3.3 (3.7), H: 0.7 (0.6), N: 2.6 (2.1).

Ag-3' was prepared by adding ca. 100 mg of crystals of **Ag-3** to ca. 1 mL of 10 M NaOH solution. The color change from pale green to black was instantaneous and the mixture was sonicated briefly to ensure all the

crystals had reacted. The resultant black material was washed three times with water, twice with ethanol, and dried in a vacuum. SEM images were obtained by dispersing the material in a small amount of ethanol and depositing onto a clean silicon wafer.

ASSOCIATED CONTENT

S Supporting Information. Crystallographic information files (CIFs) for all seven structures. General materials and methods, thermogravimetric analysis for compounds **1**, **Ag-2**, **Ag-3**, IR scans for compounds **1**, **Ag-2**, **Ag-3**, a mass spectrometry study of compound **TBA-3** and PXRD patterns for materials **Ag-2'** and **Ag-3'** are also shown. This material is available free of charge via the Internet at <http://pubs.acs.org>.

AUTHOR INFORMATION

Corresponding Author

*Fax: (+44) 141-330-4888. E-mail: L.Cronin@chem.gla.ac.uk. Homepage: <http://www.croninlab.com>.

ACKNOWLEDGMENT

This work was supported by the EPSRC, the Leverhulme Trust, WestCHEM, and the University of Glasgow. We also greatly acknowledge Prof. Dr. Paul Kögerler, Institut für Anorganische Chemie, Aachen, for ICP-OES analysis.

REFERENCES

- (1) Biswas, A.; Eilers, H.; Hidden, F.; Aktas, O. C.; Kiran, C. V. S. *Appl. Phys. Lett.* **2006**, *88*, No. 013103.
- (2) Nie, S. M.; Emery, S. R. *Science* **1997**, *275* (5303), 1102–1106.
- (3) Sun, Y. G.; Xia, Y. N. *Science* **2002**, *298* (5601), 2176–2179.
- (4) Wang, Z. L. *J. Phys. Chem. B* **2000**, *104* (6), 1153–1175.
- (5) Barnett, S. A.; Champness, N. R. *Coord. Chem. Rev.* **2003**, *246* (1–2), 145–168.
- (6) Pease, A. R.; Jeppesen, J. O.; Stoddart, J. F.; Luo, Y.; Collier, C. P.; Heath, J. R. *Acc. Chem. Res.* **2001**, *34* (6), 433–444.
- (7) Long, D. L.; Burkholder, E.; Cronin, L. *Chem. Soc. Rev.* **2007**, *36* (1), 105–121.
- (8) Long, D. L.; Tsunashima, R.; Cronin, L. *Angew. Chem., Int. Ed.* **2010**, *49* (10), 1736–1758.
- (9) Müller, A.; Beckmann, E.; Bogge, H.; Schmidtman, M.; Dress, A. *Angew. Chem., Int. Ed.* **2002**, *41* (7), 1162–1167.
- (10) Liu, T. B. *J. Am. Chem. Soc.* **2003**, *125* (2), 312–313.
- (11) Streb, C.; Tsunashima, R.; MacLaren, D. A.; McGlone, T.; Akutagawa, T.; Nakamura, T.; Scandurra, A.; Pignataro, B.; Gadegaard, N.; Cronin, L. *Angew. Chem., Int. Ed.* **2009**, *48* (35), 6490–6493.
- (12) Abbas, H.; Pickering, A. L.; Long, D. L.; Kögerler, P.; Cronin, L. *Chem.—Eur. J.* **2005**, *11* (4), 1071–1078.
- (13) Abbas, H.; Streb, C.; Pickering, A. L.; Neil, A. R.; Long, D. L.; Cronin, L. *Cryst. Growth Des.* **2008**, *8* (2), 635–642.
- (14) Song, Y. F.; Abbas, H.; Ritchie, C.; McMillan, N.; Long, D. L.; Gadegaard, N.; Cronin, L. *J. Mater. Chem.* **2007**, *17* (19), 1903–1908.
- (15) Streb, C.; Ritchie, C.; Long, D. L.; Kögerler, P.; Cronin, L. *Angew. Chem., Int. Ed.* **2007**, *46* (40), 7579–7582.
- (16) Jansen, M. *Angew. Chem., Int. Ed.* **1987**, *26* (11), 1098–1110.
- (17) Pyykkö, P. *Chem. Rev.* **1997**, *97* (3), 597–636.
- (18) Gao, G. G.; Cheng, P. S.; Mak, T. C. W. *J. Am. Chem. Soc.* **2009**, *131* (51), 18257–18259.
- (19) Pang, H. J.; Peng, J.; Sha, J. Q.; Tian, A. X.; Zhang, P. P.; Chen, Y.; Zhu, M. *J. Mol. Struct.* **2009**, *921* (1–3), 289–294.
- (20) Sha, J.; Peng, J.; Lan, Y. A.; Su, Z. M.; Pang, H. J.; Tian, A. X.; Zhang, P. P.; Zhu, M. *Inorg. Chem.* **2008**, *47* (12), 5145–5153.
- (21) Sha, J. Q.; Peng, J.; Li, Y. G.; Zhang, P. P.; Pang, H. J. *Inorg. Chem. Commun.* **2008**, *11* (8), 907–910.
- (22) Zhao, X. L.; Mak, T. C. W. *Inorg. Chem.* **2010**, *49* (8), 3676–3678.
- (23) McGlone, T.; Streb, C.; Long, D. L.; Cronin, L. *Adv. Mater.* **2010**, *22*, 4275–4279.
- (24) Wilson, E. F.; Abbas, H.; Duncombe, B. J.; Streb, C.; Long, D. L.; Cronin, L. *J. Am. Chem. Soc.* **2008**, *130* (42), 13876–13884.
- (25) Qiao, J.; Shi, K.; Wang, Q. M. *Angew. Chem., Int. Ed.* **2010**, *49* (10), 1765–1767.
- (26) Jin, H.; Wang, X. L.; Qi, Y. F.; Wang, E. B. *Inorg. Chim. Acta* **2007**, *360* (10), 3347–3353.
- (27) Soumahoro, T.; Burkholder, E.; Ouellette, W.; Zubieta, J. *Inorg. Chim. Acta* **2005**, *358* (3), 606–616.
- (28) Wang, J. P.; Zhao, J. W.; Niu, J. Y. *J. Mol. Struct.* **2004**, *697* (1–3), 191–198.
- (29) Krebs, B.; Klein, R. in: Pope, M. T.; Müller, A., Eds.; *Polyoxometalates: From Platonic Solids to Anti-Retroviral Activity*; Kluwer Academic Publishers: Dordrecht, 1994; p 55.
- (30) Jeannin, Y.; Martinfrere, J. *Inorg. Chem.* **1979**, *18* (11), 3010–3014.
- (31) Ozawa, Y.; Sasaki, Y. *Chem. Lett.* **1987**, No. 5, 923–926.
- (32) Mbomekalle, I. M.; Keita, B.; Lu, Y. W.; Nadio, L.; Contant, R.; Belai, N.; Pope, M. T. *Eur. J. Inorg. Chem.* **2004**, No. 2, 276–285.
- (33) Long, D. L.; Abbas, H.; Kögerler, P.; Cronin, L. *Angew. Chem., Int. Ed.* **2005**, *44* (22), 3415–3419.
- (34) Long, D. L.; Kögerler, P.; Cronin, L. *Angew. Chem., Int. Ed.* **2004**, *43* (14), 1817–1820.
- (35) Jorris, T. L.; Kozik, M.; Baker, L. C. W. *Inorg. Chem.* **1990**, *29* (22), 4584–4586.
- (36) Long, D. L.; Kögerler, P.; Parenty, A. D. C.; Fielden, J.; Cronin, L. *Angew. Chem., Int. Ed.* **2006**, *45* (29), 4798–4803.
- (37) Long, D. L.; Song, Y. F.; Wilson, E. F.; Kögerler, P.; Guo, S. X.; Bond, A. M.; Hargreaves, J. S. J.; Cronin, L. *Angew. Chem., Int. Ed.* **2008**, *47* (23), 4384–4387.
- (38) *PowderCell for Windows*, Version 2.4; Kraus, W.; Nolze, G., Eds.; Federal Institute for Materials Research and Testing: Berlin, Germany, 2000.
- (39) Wang, J. P.; Ma, P. T.; Zhao, J. W.; Niu, J. Y. *Inorg. Chem. Commun.* **2007**, *10* (5), 523–526.
- (40) Long, D. L.; Streb, C.; Song, Y. F.; Mitchell, S.; Cronin, L. *J. Am. Chem. Soc.* **2008**, *130* (6), 1830–1832.
- (41) Bosing, M.; Loose, I.; Pohlmann, H.; Krebs, B. *Chem.—Eur. J.* **1997**, *3* (8), 1232–1237.
- (42) Loose, I.; Droste, E.; Bosing, M.; Pohlmann, H.; Dickman, M. H.; Rosu, C.; Pope, M. T.; Krebs, B. *Inorg. Chem.* **1999**, *38* (11), 2688–2694.
- (43) Long, D. L.; Abbas, H.; Kögerler, P.; Cronin, L. *J. Am. Chem. Soc.* **2004**, *126* (43), 13880–13881.
- (44) Long, D. L.; Brücher, O.; Streb, C.; Cronin, L. *Dalton Trans* **2006**, No. 23, 2852–2860.
- (45) McGlone, T.; Streb, C.; Long, D. L.; Cronin, L. *Chem. Asian J.* **2009**, *4* (10), 1612–1618.
- (46) Zeng, L.; Chen, Y. Q.; Liu, G. C.; Zhang, J. X. *J. Mol. Struct.* **2009**, *930* (1–3), 176–179.
- (47) Klemperer, W. G.; Yaghi, O. M. *Inorganic Syntheses*; John Wiley & Sons: New York, 1990; p 27.
- (48) Sheldrick, G. M. *Acta Crystallogr., Sect. A* **2008**, *64*, 112–122.
- (49) Farrugia, L. J. *J. Appl. Crystallogr.* **1999**, *32*, 837–838.